



UNIVERSITY OF LEEDS

This is a repository copy of *Hammerstein model for hysteresis characteristics of pneumatic muscle actuators*.

White Rose Research Online URL for this paper:
<http://eprints.whiterose.ac.uk/145486/>

Version: Accepted Version

Article:

Ai, Q, Peng, Y, Zuo, J et al. (2 more authors) (2019) Hammerstein model for hysteresis characteristics of pneumatic muscle actuators. *International Journal of Intelligent Robotics and Applications*, 3 (1). pp. 33-44. ISSN 2366-5971

<https://doi.org/10.1007/s41315-019-00084-5>

(c) 2019, Springer Nature Singapore Pte Ltd. This is an author produced version of a paper published in the *International Journal of Intelligent Robotics and Applications*. Uploaded in accordance with the publisher's self-archiving policy.

Reuse

Items deposited in White Rose Research Online are protected by copyright, with all rights reserved unless indicated otherwise. They may be downloaded and/or printed for private study, or other acts as permitted by national copyright laws. The publisher or other rights holders may allow further reproduction and re-use of the full text version. This is indicated by the licence information on the White Rose Research Online record for the item.

Takedown

If you consider content in White Rose Research Online to be in breach of UK law, please notify us by emailing eprints@whiterose.ac.uk including the URL of the record and the reason for the withdrawal request.



eprints@whiterose.ac.uk
<https://eprints.whiterose.ac.uk/>

Hammerstein Model for Hysteresis Characteristics of Pneumatic Muscle Actuators

Qingsong Ai¹, Yuan Peng¹, Jie Zuo¹, Wei Meng^{1,2*}, Quan Liu¹

¹School of Information Engineering, Wuhan University of Technology, 122 Luoshi Road, Wuhan, China

²School of Electronic and Electrical Engineering, University of Leeds, LS2 9JT, Leeds, United Kingdom

Abstract—As a kind of novel compliant actuators, pneumatic muscle actuators (PMAs) have been recently used in wearable devices for rehabilitation, industrial manufacturing and other fields due to their excellent actuation characteristics such as high power/weight ratio, safety and inherent compliance. However, the strong nonlinearity and asymmetrical hysteresis cause difficulties in implementing accurate trajectory control for robots actuated by PMAs. In this paper, a method for hysteresis modeling of PMA based on Hammerstein model is proposed, which introduces the BP neural network into the hysteretic system. In order to overcome the limitation of BP neural network's single-valued mapping, an extended space input method is adapted while the Modified Prandtl-Ishlinskii model is applied to characterize the hysteretic phenomenon. A conventional PID control is implemented to track the trajectory of PMA with and without the feed-forward hysteresis compensation based on Hammerstein model, and experimental results validate the effectiveness of the designed model which has the advantages of high precision and easy identification.

Keywords—pneumatic muscle actuator, Hammerstein model, Prandtl-Ishlinskii model, asymmetric hysteresis

1. Introduction

As a new type of biomechanical soft actuator, the pneumatic muscle actuator (PMA) plays a key role in rehabilitation fields or bionic robots due to its characteristics of high power/weight ratio, safety and flexibility [1]. By applying a certain internal pressure to the PMA, it generates displacement and contraction force, under which condition that displacement and contraction force are closely related to the internal pressure. However, the displacement of the PMA during the inflation and deflation is not completely consistent with the internal pressure which is referred to as length/pressure hysteresis characteristic [2]. One of the reasons why the PMAs-driven system has strong nonlinearity is precisely because of the hysteresis characteristics, which makes the precise trajectory control or force tracking control of the system increasingly difficult. In order to eliminate the nonlinearity caused by hysteresis, an accurate hysteresis model of the PMA needs to be established.

There are many models for hysteresis characteristic of PMAs which can be roughly divided into two categories: one includes Preisach model [3], Krasnosel'skii-Pokrovskii (KP) model [4], Prandtl-Ishlinskii (PI) model [5], Maxwell-slip model [6] and its modified version [7]; they are phenomenological operator-based models, which adopt different types of mathematical operators to characterize hysteresis loops. And the other are differential-based hysteresis models, which employ nonlinear differential equations to simulate hysteresis dynamics [8], including Dahl model [9], LuGre model [10], Duhem model [11], Bouc-Wen model [12] and its variation [13]. Among the above models, the Preisach model is the most widely used, and is suitable for various hysteretic actuators, such as electromagnetic actuators [14], piezoelectric ceramic actuators [15], and magnetostrictive actuators [16]. Nevertheless, its mathematical form is very complex, which causes difficulties in deducing its inverse model. In contrast, the PI model, as a subclass of the Preisach model, is obtained by linear weighted superposition of a finite number of simple play operators, which facilitates the calculation of the inverse hysteresis model [17]. On the other hand, due to the symmetry of classical play operator [18], the classical PI (CPI) model is not suitable for asymmetric hysteretic system. In order to compensate for the shortcomings of the CPI model, Kuhnen [19] designed a modified PI (MPI) model by combining linear play operators with dead-zone (DZ) operators, which can describe asymmetric hysteresis and extend the application scope of the model. On the basis of MPI model, Xie *et al.* [20] proposed an MGPI model by adding an envelope to the input signal, which reduced the maximum error of the model to 3.0506 mm. But the complexity of the model was increased at the same time. Through comprehensive consideration of the above factors, the MPI model is adopted as the basic hysteresis operator for PMAs modeling in this paper. The Hammerstein model is composed of static nonlinear part and dynamic linear part in series, which is very suitable for describing hysteretic nonlinear system [21]. Taking advantages of Hammerstein model's simple structure and less parameters, we apply it to the study for hysteresis characteristics of PMAs. Many scholars have devoted themselves to studying the hysteresis with Hammerstein model of rigid actuators such as electromagnetic and piezoelectric ceramics. But in recent years, there have been few researches on the hysteresis modeling of PMAs with Hammerstein model.

Due to the development of artificial neural network and fuzzy logic, the method of applying neural network [22] to system modeling has appeared in recent years, whose single value mapping limits its application in the field of hysteretic system. In this paper, the MPI model is adopted to accomplish the mapping relationship between the input and output of hysteretic system, and then the multivalued mapping of hysteretic system is transformed into single value mapping combined with the input information, which realizes the introduction of neural network into the research of hysteretic system, and improves the accuracy of single MPI model. The structure of the Hammerstein model constructed in this paper is illustrated in Fig.1, where $u(t)$ denotes the pressure signal of the PMA, $x(t)$ is the output of the static nonlinear model and the input of the dynamic linear model at the same time, $y_H(t)$ is the output of Hammerstein model, which refer to the displacement of the PMA under the corresponding pressure signal. The static nonlinear part of the model adopts BP network combined with MPI model, which can fully describe the hysteresis characteristics of PMAs and improve the accuracy of the model. And the ARX model is used as the dynamic linear part.

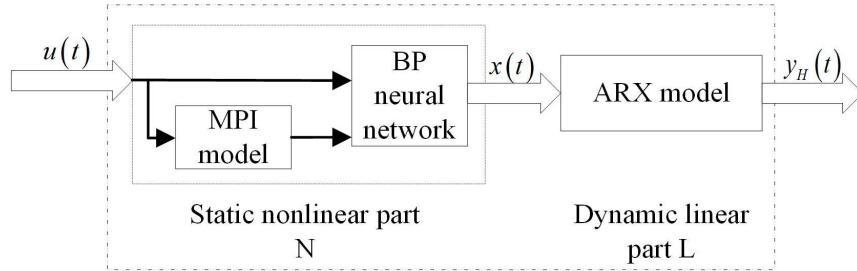


Figure 1. The structure of Hammerstein model.

The configuration of this paper is organized as follows: Section 2 illustrates the principle and derivation process of Hammerstein model in detail. In Section 3, the experiments are carried out to identify the parameters of the model and verify the effectiveness of the model. The control strategy is carried out to verify the validity of the proposed model in Section 4. Section 5 draws conclusions from the current research.

2. Hammerstein Model

The Hammerstein model is generally divided into two parts, including the static nonlinear part and the dynamic linear part. And the former is composed of MPI model as basic hysteresis operator and BP neural network. In order to overcome the limitation of single mapping relationship between neural network input and output, a method of extending the input space dimension of neural network is utilized to obtain higher accuracy in modeling of asymmetric hysteresis characteristics. This section represents the components of the Hammerstein model in turn.

2.1 BP Neural Network

Artificial neural network [22] is a dynamic system formed by a combination of many neurons with strong ability of self-learning, which can achieve nonlinear fitting between input and output. Increasing attention has been paid to the neural network that is appropriate for the modeling of complex systems, among which Back Propagation (BP) neural network is the most common one.

It is known that neural network is suitable not only for mapping between signal input and signal output, but also for mapping between multiple input and multiple output. Besides, the high precision approximation capability of neural network is very suitable for the modeling of hysteretic nonlinear system. However, it is hard for BP neural network to successfully and accurately complete the mapping relationship between signal input and multiple output in hysteretic system, which restricts the application of BP neural network in this modeling. Through further study of hysteretic characteristics, it can be found that with the trend of the input and output of the system and the information such as the historical extreme points, it is not difficult to determine the exclusive output value which is corresponding to the input signal. In this paper, MPI model is adopted to characterize the asymmetric hysteresis phenomenon of PMAs, and to distinguish the direction and trend of hysteresis curve. The input of BP neural network composes of the input signal of the system and the output of MPI model under the corresponding input signal simultaneously, which is referred to as the expansion of the input space, and determines the unique

output value of the hysteretic system. The MPI model and BP neural network constitute the static nonlinear part of Hammerstein model together as shown in Fig.1.

The static nonlinear model can be presented in the form of:

$$x(t) = f[u(t), y_D(t)] \quad (1)$$

where $u(t)$ denotes the input signal of hysteretic system which is the pressure signal of the PMA, $y_D(t)$ is the output of MPI model, $f[\square]$ represents the transmission function of BP neural network and $x(t)$ is the output of the static nonlinear model. The structure of BP neural network is shown in Fig.2. The input layer of BP neural network is 2-dimensional array, the output layer is 1-dimensional array, and the hidden layers adopt 2 layers. The first layer includes 5 neurons, and the second layer contains 10 neurons.

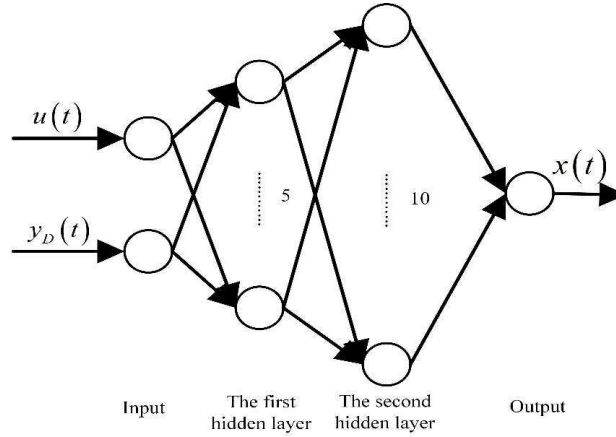


Figure 2. The structure of BP neural network.

2.2 MPI Model

In the static nonlinear model, the MPI model is adopted to simulate the asymmetric hysteresis characteristics of PMAs. Based on the CPI model, the MPI model expands the application scope of this model by utilizing the DZ operator. The CPI model can be expressed as [23], which is shown in Fig.3:

$$y_c(t) = \sum_{i=1}^n \omega_{ci} y_i(t) = \omega_c^T H_r[u(t), y_0] \quad (2)$$

$$y_i(t) = \max\{u(t) - \lambda_i, \min\{u(t) + \lambda_i, y_i(t-1)\}\} \quad (3)$$

Its initial state performs as follows:

$$y_i(0) = \max\{u(0) - \lambda_i, \min\{u(0) + \lambda_i, 0\}\} \quad (4)$$

where H_r denotes the linear operator, n is the number of operators, u and y_c represent the input and output of CPI model, respectively. y_0 denotes the initial state, $\omega_c = [\omega_{c1}, \dots, \omega_{cn}]^T$ and $\lambda = [\lambda_1, \dots, \lambda_n]^T$ are the weighted vector and the threshold vector. When the value of n increases, the parameters of the model which is noted to be $2n$ increase correspondingly, which increases the difficulty of modeling. In order to reduce the unknown parameters of the model, the i th threshold and the weighted value can be set as:

$$\begin{cases} \lambda_i = \beta i \\ \omega_{ci} = \delta e^{-\mu \lambda_i} \end{cases} \quad (5)$$

where β , δ , μ are parameters obtained through experimental modeling.

The expression of DZ operator, which is shown in Fig.3, is as follow:

$$y(t) = S_\gamma[x](t) = S(x(t), \gamma) = \begin{cases} \max\{x(t) - \gamma, 0\}, & \gamma > 0 \\ x(t), & \gamma = 0 \\ \min\{x(t) - \gamma, 0\}, & \gamma < 0 \end{cases} \quad (6)$$

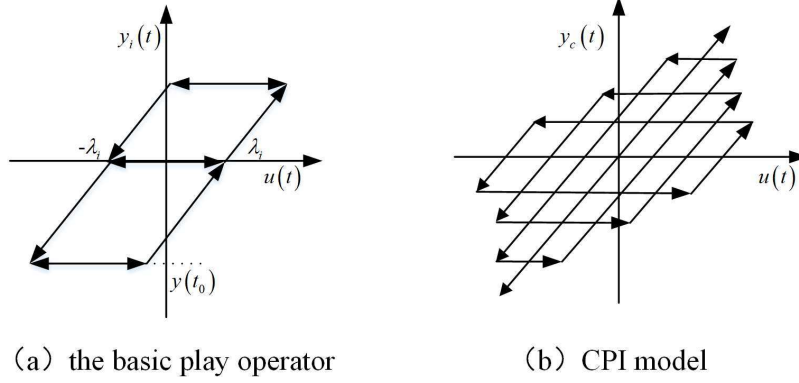


Figure 3. The structure of CPI model.

Among them, $x(t)$ and $y(t)$ are the input and output of the DZ operator respectively, whose relationship is shown in Fig.4. γ denotes the threshold value of the DZ operator which can be defined as $\gamma_j = \frac{j}{m} \max(y_c)$, $j = 0, 1, \dots, m$, where m represents the superposition number of the DZ operators. The output of DZ model can be expressed as:

$$\begin{aligned} y_s(t) &= \omega_d^T S_\gamma[x](t), \omega_d = (\omega_{d0}, \omega_{d1}, \dots, \omega_{dm})^T \\ \gamma &= (\gamma_0, \gamma_1, \dots, \gamma_m)^T \\ S_\gamma[x](t) &= (S_{\gamma_0}[x](t), S_{\gamma_1}[x](t), \dots, S_{\gamma_m}[x](t))^T \end{aligned} \quad (7)$$

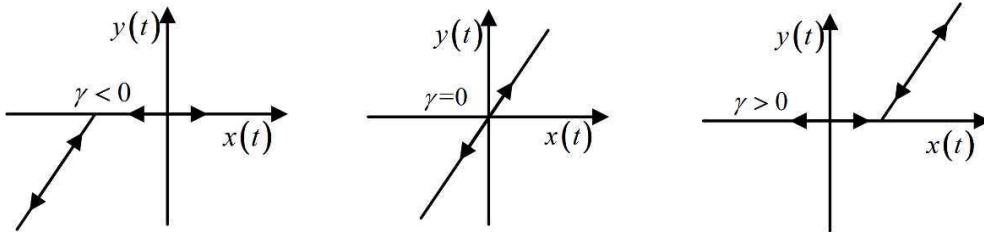


Figure 4. The structure of DZ operator.

Substituting (2) into (5), the MPI model, which is shown in Fig.5, can be written as:

$$y_D(t) = \Gamma[u](t) = \omega_d^T S_\gamma[\omega_c^T H_r(u, y_0)](t) \quad (8)$$

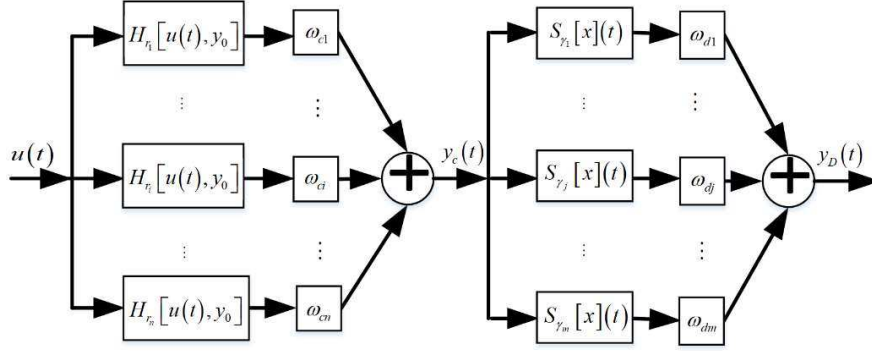


Figure 5. The structure of MPI model.

2.3 ARX Model

The AutoRegressive eXogenous (ARX) model is a rational transfer function model, which is widely used in system identification. In this paper, it is used to represent the dynamic linear part of Hammerstein model. ARX mathematical expression is as follows:

$$A(z)y(t) = B(z)x(t) \quad (9)$$

$$H(z) = \frac{B(z)}{A(z)} \quad (10)$$

where $x(t)$ and $y(t)$ are the input and output of the model respectively, $A(z), B(z)$ are the polynomial to be solved, and $H(z)$ denotes the transfer function of the ARX model. The Hammerstein model can be expressed as:

$$y_H(t) = H(z) \cdot f[u(t), \omega_d^T S_d[\omega_c^T H_r(u, y_0)](t)] \quad (11)$$

Moreover, the inverse Hammerstein model can be obtained from the inverse MPI model shown in equation (12)

$$u(t) = \omega_c^T H_r'[\omega_d^T S_\gamma'(y_D)](t) \quad (12)$$

$$u(t) = f'[y_H(t) \square H(z)^{-1}, \omega_c^T H_r'[\omega_d^T S_\gamma'(y_D)](t)] \quad (13)$$

$$\begin{cases} \lambda'_i = \lambda_i + \sum_{j=1}^{i-1} \omega_{cj} (\lambda_i - \lambda_j), i = 0, 1, \dots, n \\ \omega'_{ci} = \frac{-\omega_{ci}}{\left(1 + \sum_{j=1}^i \omega_{cj}\right) \left(1 + \sum_{j=1}^{i-1} \omega_{cj}\right)}, i = 0, 1, \dots, n \\ \gamma'_j = \sum_{k=0}^j \omega_{dk} (\gamma_j - \gamma_k), j = 0, 1, \dots, m \\ \omega'_{dj} = \frac{-\omega_{dj}}{\left(\sum_{k=0}^j \omega_{dk}\right) \left(\sum_{k=0}^{j-1} \omega_{dk}\right)}, j = 0, 1, \dots, m \end{cases} \quad (14)$$

3 Hysteresis Characteristics of PAMs

3.1 Experiment Platform

The length/pressure hysteresis characteristics of PAMs can be identified by isobaric experiment, with the hardware configuration as shown in Fig.6. It includes PMA (FESTO DMSP-20-400N), displacement transducer (MLO-POT-TLF), load cell, air proportional valve (ITV 2050-212N), A/D and D/A data acquisition card, host computer and air pump. One end of the PMA, which is connected to the trachea, is fixed to the base and the other end is connected to the external load. The internal pressure of the PMA is controlled by an air proportional valve. The displacement of the PMA are measured by a displacement

transducer, and the sensing data are collected and then transmitted to the host computer through A/D data acquisition card. And then through the conversion of D/A data, the control signal from the host computer performs as the input signal of the proportional valve, which changes the internal pressure of the PMA. The length/pressure hysteresis characteristics can be obtained according to the displacement data under different pressure.

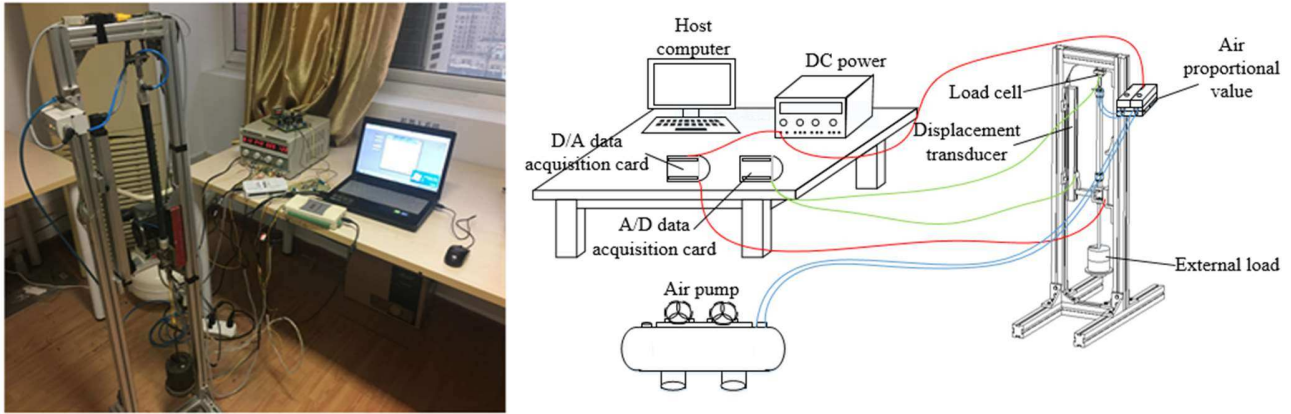


Figure 6. The experimental platform for PMA.

The experimental steps are as follows: In the initial state, the internal pressure and the displacement of the PMA are both zero, and the PMA is at the initial length. The control signal derives from different triangular waveforms with different amplitudes, whose amplitudes increases gradually from 0 bar to 4 bar ($1\text{bar} = 1 \times 10^5 \text{Pa}$) with each step of 1 bar. Through recording the position information of the PMA during the experiment, the relationship of length/air pressure hysteresis under different pressure is obtained. Subsequently, by changing the external load of the PMA, the relationship between length/pressure hysteresis of PMA and external load can be obtained through experimental data.

3.2 Length/Pressure Hysteresis Phenomenon

After comprehensive analysis of experimental data, the length/pressure hysteresis curve can be obtained which is depicted in Fig.7 under the zero load condition. Fig.7 (a) illustrates the hysteresis curve through repeated experiments, which suggests that the system exits dithering error and there may be contingency in a single experiment. Therefore, the mean value calculated from multiple sets of experimental data is set to represent its hysteresis characteristics as shown in Fig.7 (b). Fig.8 (a)-(d) illustrate the hysteresis curves with external load of 1.5 kg, 3.5 kg, 5.5 kg and 7.5 kg respectively. The hysteresis curves with different external load at the same pressure are compared in Fig.9.

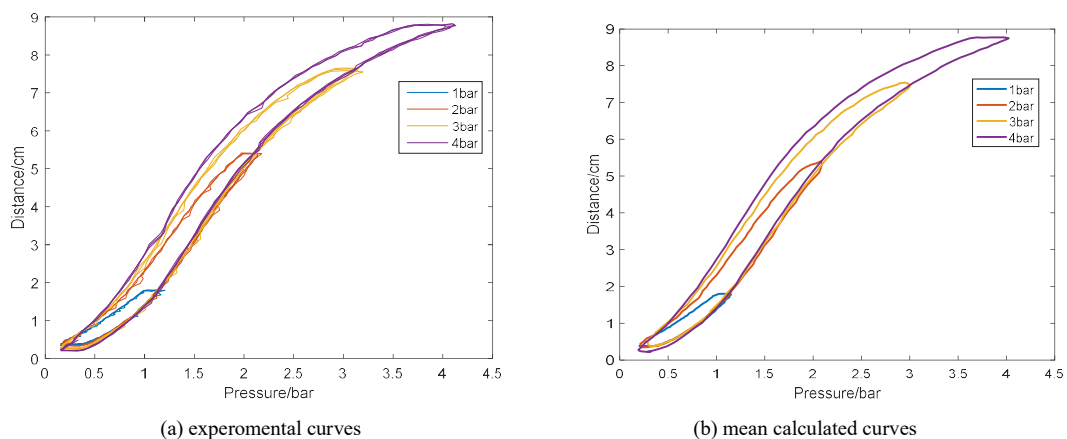


Figure 7. Hysteresis curves without external load.

As can be clearly seen from Fig.7, the displacements of the PMA under the same internal pressure during inflation and deflation are different, which is referred to as a hysteresis loop. The hysteresis loop formed under the maximum input pressure

signal is called the main loop, in which the loops are called the secondary loops. The measured data of the main loop are used to identify the parameters of the Hammerstein model. The hysteresis curve trend under different external loads shown in Fig.8 is consistent with the hysteresis curve without external load, indicating that the external load does not change the inherent hysteresis curve of the PMA.

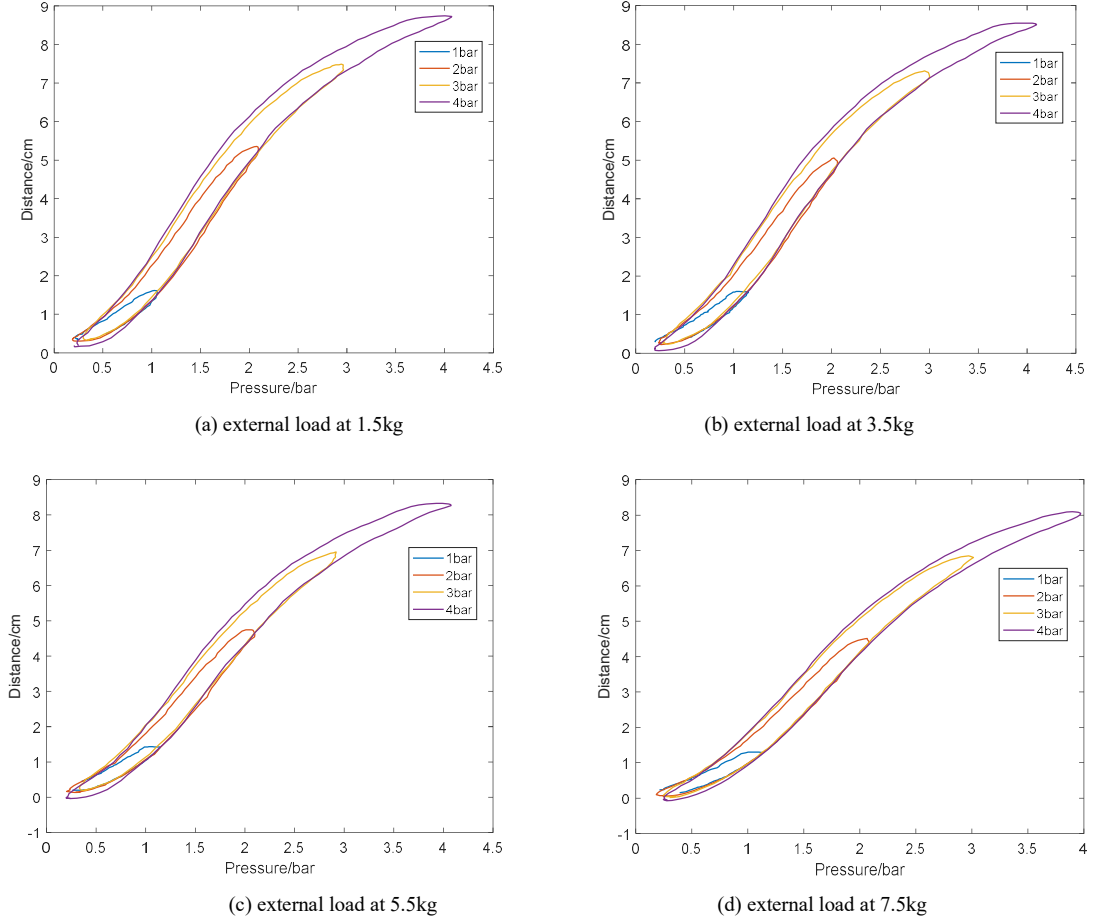


Figure 8. Hysteresis curves at different external load.

Sarosi et al. [24] established the static contraction model and designed a function simulation for the force generated by PMAs. The contraction force was calculated by the internal pressure and contraction rate of PMAs which can be presented as:

$$F(p, \varepsilon) = (p + a) \cdot e^{b \cdot \varepsilon} + c \cdot p \cdot \varepsilon + d \cdot p + e \quad (15)$$

$$p(\varepsilon, F) = \frac{F - a \cdot e^{b \cdot \varepsilon} - e}{e^{b \cdot \varepsilon} + c \cdot \varepsilon + d} \quad (16)$$

Among them, F, p, ε represent the contraction force, the internal pressure and contraction rate of a PMA respectively, and a, b, c, d, e are the model parameters to be solved. When the displacement of the PMA remains constant, the pressure increases with the increase of the contraction force. Fig.9 compares the hysteresis curves with different external load at the same pressure of 4 bar and points out that under the same displacement, the greater the external load, the greater the pressure value. This phenomenon can be satisfied both during the process of inflation and deflation. In this experiment, different external loads can be equivalent to the effect contraction force.

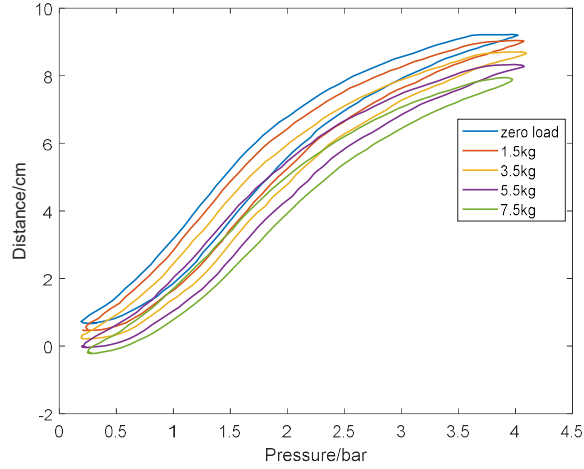


Figure 9. Hysteresis curves with different external loads at 4 bar.

3.3 Model Identification and Validation

The inherent high nonlinearity, time-varying and hysteresis of the PMA cause difficulties in parameter identification. The nonlinear least squares algorithm is widely used in parameter estimation, which can find the optimal coefficient by minimizing the weighted cost function of the measured data [22].

The Hammerstein model consists of two parts, so it is necessary to identify the MPI model and ARX model separately in two steps. Firstly, the identification of the static hysteretic nonlinear module, which is mainly referred to MPI model, is carried out. An input signal with a frequency of 0.05 HZ is given on the experimental platform, and the position information of a PMA is collected. The parameters of MPI model are identified by the least squares method, under which condition the dynamic linear module is equal to 1. Afterwards, the parameters of dynamic linear module are identified. The order of ARX model is mainly determined by using AIC (Akaike's information criterion) and the order of this system is determined to be the best at 2.

It should be pointed out that the more the play operators and the DZ operators, the higher the accuracy of the MPI model, but at the same time, more calculations are needed. After comprehensive consideration, this experiment takes 20 play operators and 20 DZ operators, and the results of parameter identification are shown in Table 1 and 2. The identification results of ARX model are as follows:

$$H(z) = \frac{0.9845z - 0.4851}{z^2 - 0.5243z - 1.2471} \quad (17)$$

Table 1. Parameter identification results of MPI model

β	δ	μ
0.0766	0.8335	4.8410

Table 2. Parameter identification of DZ model

i	1	2	3	4	5	6	7	8	9	10
ω_{di}	0.102	0.17	0.0792	0.04	0.11	0.12	-0.113	-0.013	0.0377	-0.0812
		75		52	30	96				
i	11	12	13	14	15	16	17	18	19	20
ω_{di}	-0.042	0.01	-0.055	0.06	0.01	0.01	-0.032	-0.023	0.0168	-0.0129
		5		8	71	58				

To fully confirm the effectiveness of the proposed model, the results of experimental verification of MPI model and Hammerstein model are respectively illustrated in Fig.10 and Fig.11, which compare the simulation results with the experimental length/hysteresis curve of PMA. From Fig.10 (a), it can be intuitively seen that the fitting effect of the MPI

model is not good and the maximum error reaches 0.8524cm. There exists a bit large modeling error in fitting hysteresis characteristic curve using MPI model as shown in Fig.10 (b) which is almost 10 times bigger than modeling error of Hammerstein model. On the other hand, it can be seen from Fig.11 (a) that the model simulation and experimental curves fit perfect which means that the Hammerstein model performs excellently in characterizing the hysteresis of PMAs. In order to eliminate the contingency in a single experimental result, 20 sets of experimental data are taken and corresponding model simulations are compared to obtain the mean absolute error (MAE) under each input pressure and the standard deviation (STD) which denotes the degree of deviation from the mean value, which are shown in Fig.11 (b). From Fig.11 (b), we can know that the maximum MAE under input pressure values is 0.438 mm, and the maximum deviation from the average value is no more than 0.8 mm. In the literature [20] mentioned in the Introduction, the MGPI model is used to simulate the hysteresis characteristics of a PMA, and the maximum error reaches 3.0506 mm, which further proves the validity of the Hammerstein model for high-precision modeling for hysteresis characteristics of PMAs. Comparing Fig.10 with Fig.11, it is clear that the BP neural network plays an importance role in the structure of Hammerstein model because of its high precision approximation capability.

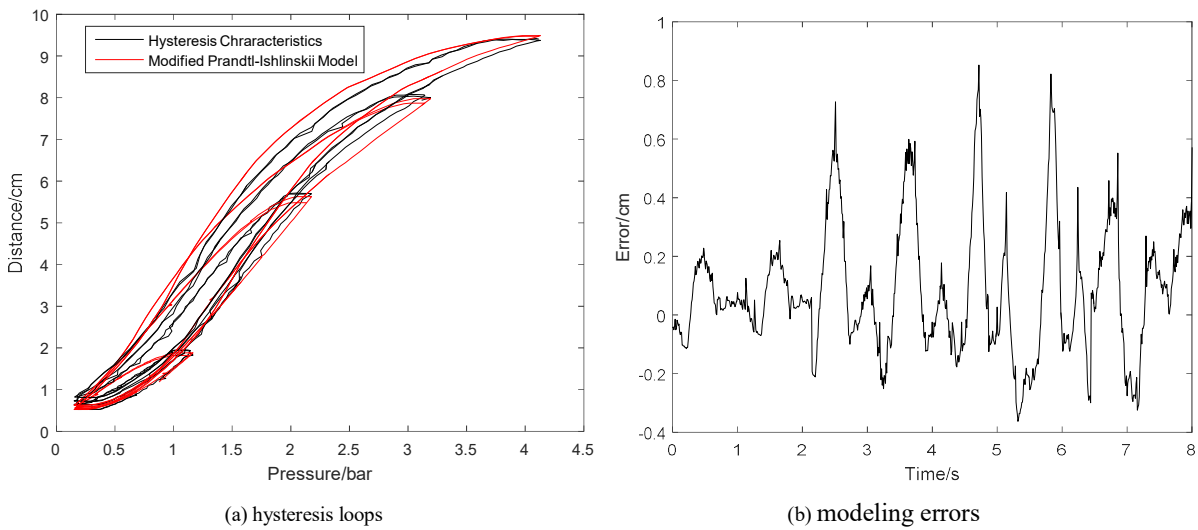


Figure 10. Model validation result of MPI model.

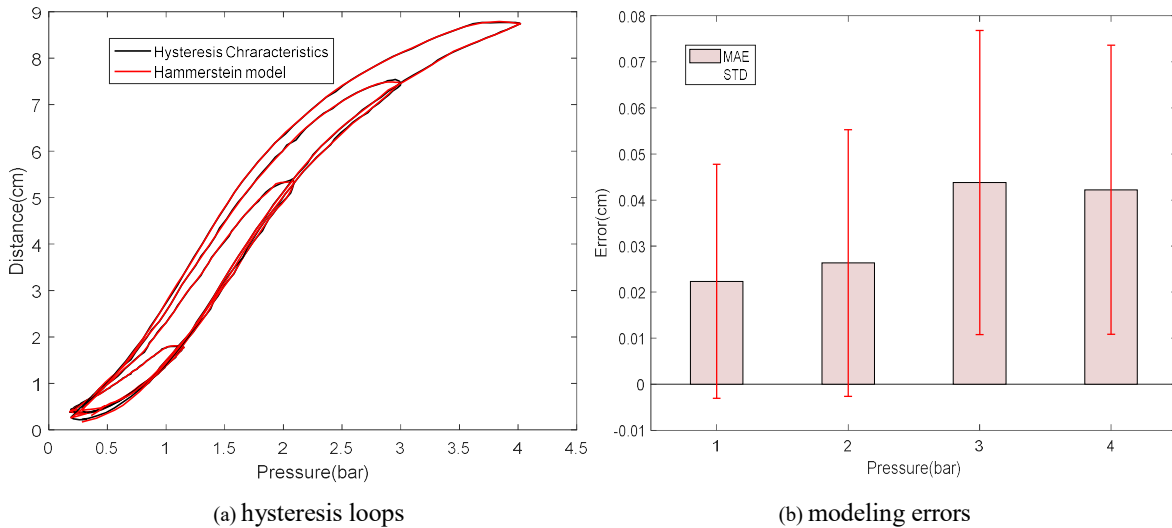


Figure 11. Model validation result of Hammerstein model.

4. Model-based Control Experiment

To further illustrate the effect of the Hammerstein model, the feed-forward compensation based on the inverse Hammerstein model is adapted in the trajectory tracking control of PMA with PID control strategy, whose configuration is shown in Fig.12.

4.1 Controller design

A conventional PID control [25] is implemented to track the trajectory of PMA with the feed-forward hysteresis compensation which is designed to reduce the influence of the hysteresis characteristics. The inverse Hammerstein model maps the desired trajectory y_H into the desired pressure P_H for a PMA, which is then applied to the air proportional value as control signal. Therefore, the actual trajectory y_A can be collected and compared with the desired trajectory y_H . In this paper, the gains of the PID control included in the feedback loop are set in Table 3.

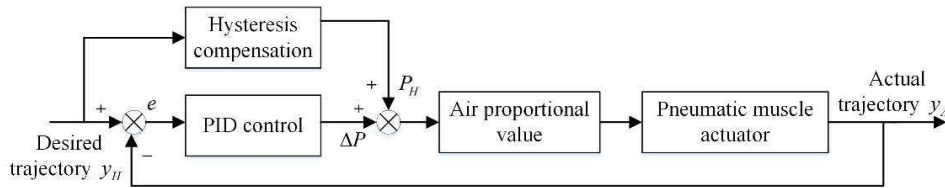


Figure 12. The control scheme for PMA.

Table 3. Controller gains for the PID control

Proportional	Integral	Differential
1	0.01	0

4.2 Experimental results

In order to testify the performance of the proposed control strategy and the effect of the hysteresis compensation based on the inverse Hammerstein model, the experiments on trajectory tracking control with and without the hysteresis compensator for a PMA is implemented and compared later. The desired tracking signal is designed as:

$$y_d(t) = A \sin(2\pi ft) + H \quad (18)$$

where A, f, H are the amplitude, the frequency and offset of the desired tracking signal, respectively, which are given in Table 4.

Table 4. Parameters of sinusoidal signal

$A[cm]$	$f[Hz]$	$H[cm]$
3	0.2	4

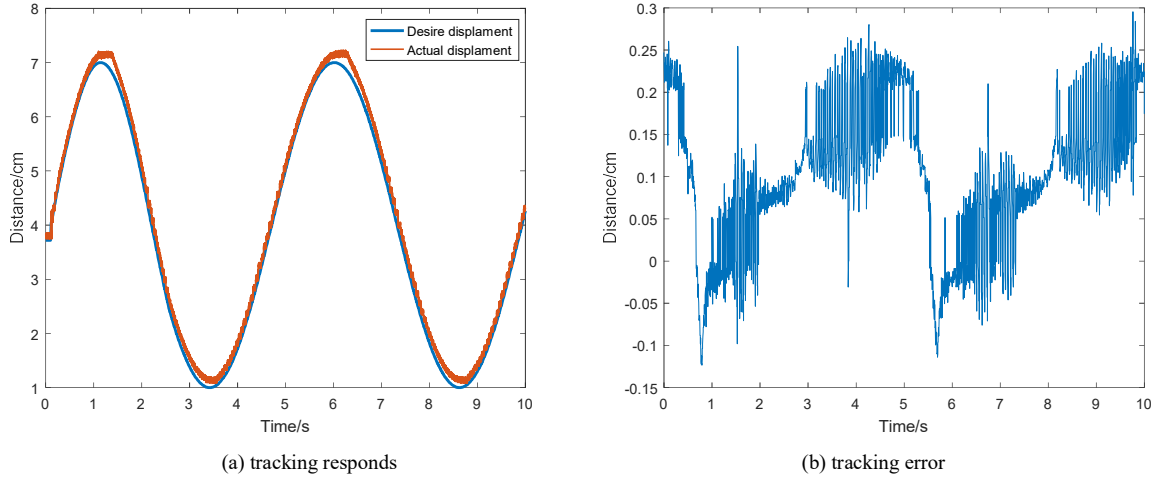


Figure 13. Results for the trajectory tracking control of the PMA without the hysteresis compensation.

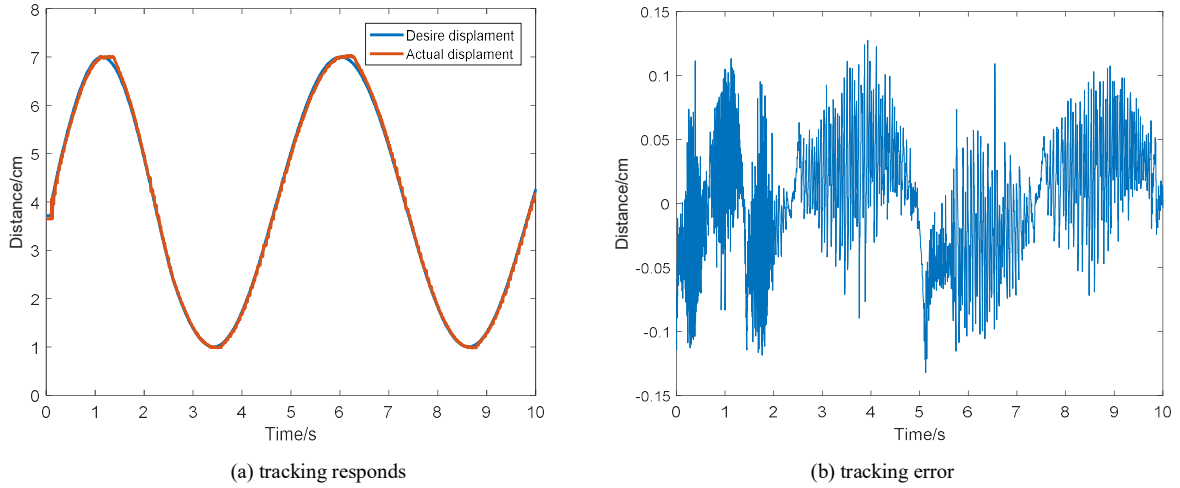


Figure 14. Results for the trajectory tracking control of the PMA with the hysteresis compensation.

Given the desired tracking signal, the results of the trajectory tracking control without and with the feed-forward hysteresis compensation based on the Hammerstein model are shown in Fig.13 and 14 respectively. Table 5 lists the statics of the trajectory tracking error. It is obvious that the tracking errors become a bit larger at peaks and troughs than that at other parts of the trajectory for both conditions. Nevertheless, by adding the hysteresis compensation into the control scheme, the performance of the trajectory tracking control becomes much better not only at peaks and troughs, but also the other parts of the trajectory achieve a more smooth movement than that of the trajectory under conventional PID control.

Table 5. The tracking errors of sinusoidal trajectory

	Maximum error [cm]	Mean absolute error [cm]	RMS error [cm]
PID	0.2952	0.0665	0.0861
PID + feed-forward	0.1319	0.0359	0.0445

It can be seen from Fig.10 and 13 that the error in the trajectory tracking control is larger than that of the simulation of the proposed model. The reason why tracking error increases compared with model error is because there exist uncertainties such as system interference under dynamic condition, moreover, the hysteresis characteristics of PMAs become more complicated. From the numerical results as shown in Table 5, it is clear that the maximal error is 0.1319 cm, the mean absolute error is 0.0359 cm and the RMS error is only 0.0445 cm, which are much smaller than those in the PID control without the

feed-forward compensator, and meanwhile are also about as half as small as those in the literature [25] under the same control scheme with the hysteresis compensation. The generalized PI (GPI) model is designed to perform as hysteresis compensation in the trajectory tracking control in literature [25]. From experimental results, the Hammerstein model performs better in compensating the influence of length/pressure hysteresis than the GPI model under same condition.

5. Conclusion

In this paper, a Hammerstein model is presented to characterize the asymmetric length/pressure hysteresis of PMAs. The proposed MPI model combines the linear play operator with the DZ operator, which extends the application of the CPI model and is suitable for representing the asymmetric hysteresis characteristics. Simultaneously utilizing the input signal of hysteresis system and the output of MPI model as the input of BP neural network, the limitation for single-valued mapping of neural network is successfully overcome, and the high-precision approximation ability of neural network is introduced into the research of hysteresis modeling of PMAs, which improves the accuracy of the model while improving the self-learning ability of the model. In order to verify the effect of the model, a conventional PID control with hysteresis compensation is carried out. And the trajectory tracking results demonstrate that the Hammerstein model and its inversion can realize high accuracy in both model simulation and trajectory control, which is significant for the applications driven by PMAs.

In order to prevent secondary injury of patients, the assistant motion of the rehabilitation robot driven by PMAs is carried out at low frequency. Therefore, it is reasonable to study the hysteresis characteristics of PMAs under quasi-static conditions. Under dynamic conditions, not only the hysteresis characteristics of PMAs will become more complicated, but also the uncertainties such as system interference will appear in real-time application, making it impossible to establish its accurate model. Moreover, there exist dithering and creep during the trajectory tracking control. Therefore, it is necessary to achieve a more intelligent control method to solve the above problems. In the future, we will focus on the control method and develop a strong robust controller to achieve more accurate trajectory control of PMAs.

Acknowledgment

This work was supported by the National Natural Science Foundation of China under Grants 51705381 and 51675389 and Nature Science Foundation of Hubei Province (2017CFB428) and Overseas S&T Cooperation.

References

- [1] Meng W, Liu Q, Zhou Z, et al. Recent development of mechanisms and control strategies for robot-assisted lower limb rehabilitation. *Mechatronics*, 2015, 31:132-145.
- [2] T Takashima K, Rossiter J, Mukai T. McKibben artificial muscle using shape-memory polymer. *Sensors and Actuators A: Physical*, 2010, 164(1-2):116-124.
- [3] Zhang B, Gupta B, Ducharme B, et al. Preisach's Model Extended With Dynamic Fractional Derivation Contribution. *IEEE Transactions on Magnetics*, 2017:1-4.
- [4] Zhou M, He S, Hu B, et al. Modified KP Model for Hysteresis of Magnetic Shape Memory Alloy Actuator. *Iete Technical Review*, 2015, 32(1):29-36.
- [5] Xie S, Mei J, Liu H, et al. *Motion Control of Pneumatic Muscle Actuator Using Fast Switching Valve// Mechanism and Machine Science*. Springer Singapore, 2017.
- [6] Vo-Minh T, Tjahjowidodo T, Ramon H, et al. A New Approach to Modeling Hysteresis in a Pneumatic Artificial Muscle Using The Maxwell-Slip Model. *IEEE/ASME Transactions on Mechatronics*, 2011, 16(1):177-186.
- [7] Y Ompusunggu A P, Sas P, Van Brussel H. Modeling and simulation of the engagement dynamics of a wet friction clutch system subjected to degradation: An application to condition monitoring and prognostics. *Mechatronics*, 2013, 23(6):700-712.
- [8] Lin C J, Lin C R, Yu S K, et al. Hysteresis modeling and tracking control for a dual pneumatic artificial muscle system using Prandtl-Ishlinskii model. *Mechatronics*, 2015, 28:35-45.
- [9] Prakash M, Shome S K, Pradhan S, et al. A comparison of dithers for hysteresis alleviation in dahl model based piezoelectric actuator// 2013 International Conference on Control, Automation, Robotics and Embedded Systems (CARE). IEEE, 2014.
- [10] Ruderman, Michael. Presliding hysteresis damping of LuGre and Maxwell-slip friction models. *Mechatronics*, 2015, 30:S0957415815001221.
- [11] Lin C J, Lin P T. Tracking control of a biaxial piezo-actuated positioning stage using generalized Duhem model. *Computers & Mathematics with Applications*, 2012, 64(5):766-787.

- [12] Ismail M, Ikhouane F, Rodellar J. The Hysteresis Bouc-Wen Model, a Survey. *Archives of Computational Methods in Engineering*, 2009, 16(2):161-188.
- [13] Sengupta P, Li B. Modified Bouc-Wen model for hysteresis behavior of RC beam-column joints with limited transverse reinforcement. *Engineering Structures*, 2013, 46(46):392-406.
- [14] Xiao S L, Li Y M. Optimal design, fabrication and control of an xy micro-positioning stage driven by electromagnetic actuators. *IEEE Transactions on Industrial Electronics*, 2013, 60(10):4613-4626.
- [15] Xiao S, Li Y. Modeling and High Dynamic Compensating the Rate-Dependent Hysteresis of Piezoelectric Actuators via a Novel Modified Inverse Preisach Model. *IEEE Transactions on Control Systems Technology*, 2013, 21(5):1549-1557.
- [16] Li Z, Su C Y, Chai T. Compensation of Hysteresis Nonlinearity in Magnetostrictive Actuators With Inverse Multiplicative Structure for Preisach Model. *IEEE Transactions on Automation Science & Engineering*, 2014, 11(2):613-619.
- [17] Aschemann H, Schindele D. Comparison of Model-Based Approaches to the Compensation of Hysteresis in the Force Characteristic of Pneumatic Muscles. *IEEE Transactions on Industrial Electronics*, 2014, 61(7):3620-3629.
- [18] Gu G Y, Zhu L M, Su C Y. Modeling and Compensation of Asymmetric Hysteresis Nonlinearity for Piezoceramic Actuators With a Modified Prandtl-Ishlinskii Model. *IEEE Transactions on Industrial Electronics*, 2013, 61(3):1583-1595.
- [19] Kuhnen K. Modeling, Identification and Compensation of Complex Hysteretic Nonlinearities: A Modified Prandtl-Ishlinskii Approach. *European Journal of Control*, 2003, 9(4):407-418.
- [20] Xie S L, Liu H T, Mei J P, et al. Modeling and compensation of asymmetric hysteresis for pneumatic artificial muscles with a modified generalized Prandtl-Ishlinskii model. *Mechatronics*, 2018(52): 49-57.
- [21] Zhang J, Chin K S, Ławryńczuk M. Nonlinear model predictive control based on piecewise linear Hammerstein models. *Nonlinear Dynamics*, 2018:1-21.
- [22] Li M, Wu H, Wang Y, et al. Modified Levenberg-Marquardt Algorithm for BP Neural Network Training in Dynamic Model Identification of Mechanical Systems. *Journal of Dynamic Systems Measurement & Control*, 2017, 139(3).
- [23] Janaideh M A, Rakheja S, Su C Y. A generalized Prandtl-Ishlinskii model for characterizing the hysteresis and saturation nonlinearities of smart actuators. *Smart Materials & Structures*, 2009, 18(4):045001.
- [24] Sarosi J. New approximation algorithm for the force of Fluidic Muscles/ *IEEE International Symposium on Applied Computational Intelligence and Informatics*. IEEE, 2012:229-233.
- [25] Mei J P, Xie S L, Liu H T, et al. Hysteresis Modelling and Compensation of Pneumatic Artificial Muscles using the Generalized Prandtl-Ishlinskii Model. *Journal of Mechanical Engineering*, 2017,63(11):657-665.